

MPI-Ph/94-85
December 1994

QCD PREDICTIONS ON MULTIPARTICLE FINAL STATES*

WOLFGANG OCHS[†]

*Max Planck Institut für Physik
Werner-Heisenberg-Institut
Föhringer Ring 6, D-80805 München*

Abstract

We compare QCD predictions with experimental data on inclusive multiparticle observables whereby we discuss various realizations of the idea of parton hadron duality which is related to a soft confinement mechanism. Special emphasis is given on effects from the running α_s , the soft gluon interference, scaling properties and the role of the limiting scale Q_0 in cascade evolution.

*Invited talk at the XXIV Int. Symp. Multiparticle Dynamics, Vietri sul Mare, Italy, Sept. 1994, to be publ. in Proc., Eds. A. Giovannini, S. Lupia and R. Ugoccioni, World Scientific, Singapore.

[†]e-mail adress: wwo@dmumpiwh.bitnet

QCD PREDICTIONS ON MULTIPARTICLE FINAL STATES

WOLFGANG OCHS

*Max-Planck-Institut für Physik
Föhringer Ring 6, 80805 München, Germany*

ABSTRACT

We compare QCD predictions with experimental data on inclusive multiparticle observables whereby we discuss various realizations of the idea of parton hadron duality which is related to a soft confinement mechanism. Special emphasis is given on effects from the running α_s , the soft gluon interference, scaling properties and the role of the limiting scale Q_0 in cascade evolution.

1. Introduction

There is a hierarchy of Perturbative QCD predictions depending on the sensitivity to the hadronization process which is not yet understood at a satisfactory level within the theory.

First there is the calculation of quantities in Perturbation theory in fixed order of α_s . These studies strongly support Perturbative QCD as the theory of strong interactions: The measurement of the total cross sections in e^+e^- or in deep inelastic lepton nucleon scattering, then the analysis of jet cross sections in hard collisions. In the latter application a (not entirely trivial) assumption has to be made on the equality of cross sections for production of hadron jets and of parton jets at the same resolution. The spectacular successes of such predictions have established the basic properties of the coupling and the vertices in PQCD at large Q^2 in terms of one scale parameter $\Lambda_{\overline{MS}}$.

Secondly, by applying the leading log approximation for the multiparton production, one can push PQCD further and resolve the more detailed intrinsic structure of jets.¹⁻⁶ An additional cutoff parameter Q_0 is introduced which regularizes the collinear and infrared singularities of the gluon bremsstrahlung processes. Predictions can be obtained on various observables of a multiparticle final state. There are two different approaches towards comparison of such calculations with experiment.

1. Parton-Hadron-Duality (PHD) in various forms.

The general idea is that a parton jet resembles in some aspects a hadron jet. An initial argument for such a behaviour was the proof of “preconfinement”, i.e. the parton cascade already in the perturbative region prepares color singlet clusters with finite mass independent of energy.⁷ However, these clusters are too heavy for realistic phenomenological applications. So one has to assume some kind of soft hadroniza-

tion mechanism which allows to compare properties of hadronic and partonic final states.^{4,5} In the application one can distinguish further

a) infrared and collinear safe observables

In this case the value of the observable doesn't change if a soft particle is added or if one particle is split into two collinear particles. Such observables are independent of the cutoff Q_0 and have therefore a chance not to depend on the final stage of the jet evolution. Quantities of this type are energy flows and -correlations, global quantities like thrust etc. (for a review, see ref. 8).

b) infrared sensitive observables

Here particles are counted. Examples are multiplicities, inclusive spectra and correlations which are discussed in particular at a multiparticle conference. These observables depend explicitly on the cutoff Q_0 and the QCD results cannot be compared to data immediately in a meaningful way.

For such quantities one may follow two strategies:

b1) One constructs again infrared safe quantities. This is possible if the Q_0 dependence factorizes so that it drops out after proper normalization. Another possibility is rescaling of variables which may lead to asymptotically safe quantities.

b2) A more progressive strategy would be to interpret Q_0 as hadron mass (say $Q_0 \sim m_\pi$) and to compare the observables for a parton jet evolved down to hadronic scales directly to the experimental data. This procedure has been shown to work for momentum spectra ("Local Parton Hadron Duality" (LPHD)¹¹).

2. Parton cascade with hadronization model.

The parton cascade evolves down to a cutoff $Q_0 > m_h$, specific models are then introduced to describe the hadronization process. Most popular are the string model by the Lund group⁹ ($Q_0 \sim 1$ GeV) and the cluster model by Marchesini and Webber¹⁰ ($Q_0 \sim 0.3$ GeV).

In this review we discuss the infrared sensitive quantities in multiparticle production. Also for such observables analytical results are important and indispensable for a deeper understanding of the QCD predictions; only then can we discuss power laws, the consequences of running α_s and scaling properties.

The QCD calculations can be carried out analytically in the simplest case in the double logarithmic approximation (DLA) which takes into account the leading contributions from the infrared and collinear divergencies and provides the asymptotic result at very high energies. The nonleading corrections are typically large and can be given by an expansion of the type $1 + a\sqrt{\alpha_s} + b\alpha_s + \dots$. Such Modified LLA (MLLA) with subleading corrections take into account, for example, energy recoil effects but not yet angular recoils (see, for example, ref. 6). Alternatively one may derive QCD results with Monte Carlo methods which are typically more accurate and can serve as an important check of the approximations of the analytical calculations.

The aim of the study of multiparticle phenomena in this context is to learn about the soft limit of QCD and color confinement, the part of the theory not well understood. In particular we are interested how the running of α_s , the soft gluon interference ("angular ordering"), various scaling properties, the limiting scale Q_0 intrinsic to the parton cascade are reflected in the observable particle distributions.

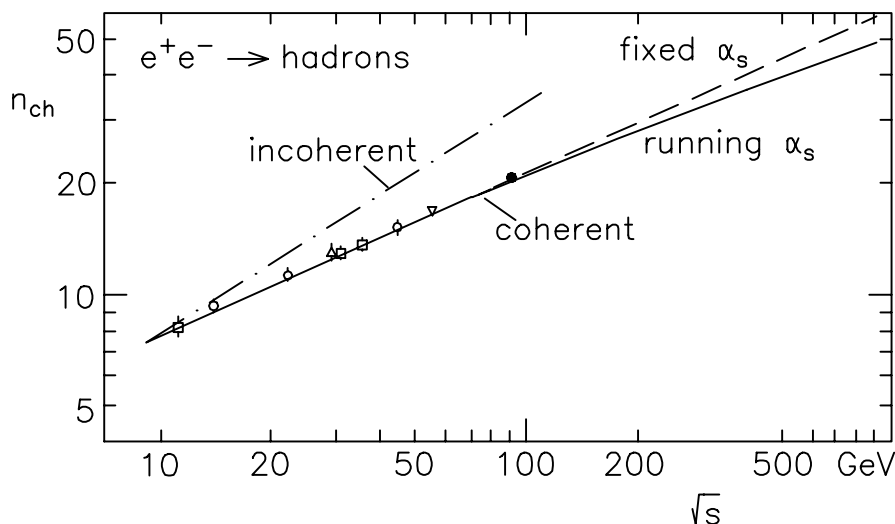


Figure 1: Average charged particle multiplicity for different CM energies \sqrt{s} and NLO QCD fit for running α_s .¹⁴ Also shown is a fit with fixed α_s (power law) and the effect of disregarding the soft gluon interference

2. Particle Multiplicities

2.1 Total Multiplicity

The multiplicity of partons emitted from a primary parton of momentum P into a cone of half opening angle Θ behaves asymptotically in QCD like

$$\bar{n} \sim c \alpha_s^b \left(\frac{P\Theta}{\Lambda} \right)^{2\gamma_0(P\Theta)} \quad (1)$$

For the full event one sets $\Theta = 1$. Here $\gamma_0 = \sqrt{6\alpha_s/\pi}$ is the QCD anomalous dimension controlling the multiplicity evolution in DLA.¹² For running α_s we have $\gamma_0^2(p_T) = \beta^2/\ln(p_T/\Lambda)$ with $\beta^2 = 12(\frac{11}{3}N_c - \frac{2}{3}N_f)^{-1}$. The prefactor comes from the NLO of the anomalous dimension¹³ and $b = 0.4916$ for $N_f = 5$. For fixed α_s the multiplicity behaves as in (1) but with constant exponent γ_0 and rises like a power with energy. For running α_s the rise is more slowly. The Q_0 dependence sits in the prefactor, therefore the ratio $n(P)/n(P_0)$ is infrared safe. Results on \bar{n} of higher accuracy and for the full energy range are also available.⁶

A fit of type (1) is shown in Fig. 1.¹⁴ The distinction between fixed and running α_s is not possible with present data but the difference will become larger at higher energies. The slope is well reproduced by QCD[†] with soft gluon interference taken into account. Neglecting the interference would increase the slope by $\sqrt{2}$ clearly inconsistent with data for any reasonable Λ parameter.

[†]For $\Lambda = 0.145$ corresponding to $\alpha_s(M_z) = 0.117$; a change of Λ by a factor of 10 would change the slope by $\sim 15\%$.)

Figure 2: The KNO multiplicity distribution in $x = n/\bar{n}$ for infinite energies (thin line) and LEP energies (thick line), calculated for a gluon jet with fixed α_s in NNLO of QCD.¹⁹ The negative binomial distribution (open points) with parameter $K = 7$ is also shown for comparison.

2.2 Multiplicity Distribution

In the DLA, valid for asymptotic energies, one derives¹⁵ a scaling property for the probability P_n in the rescaled multiplicity n/\bar{n} (“KNO-scaling”^{16,17}).

$$\bar{n}P_n = f(n/\bar{n}) \quad (2)$$

There are large corrections to the asymptotic behavior from momentum conservation alone which has been studied analytically^{18,19} and numerically.²⁰ In Fig. 2 we show as an example a calculation for a gluon jet with fixed α_s in next-to-next-to leading order.¹⁹ The asymptotic behavior for large x is exponential $f(x) \sim e^{-\beta_o x}$ (with $\beta_o \approx -2.552$). The approach to this scaling limit is very slow and the preasymptotic distribution at LEP energies looks quite different, at large x the distribution $f(x)$ drops faster, like

$$f(x) \sim \exp(-[Dx]^\mu), \quad \mu = (1 - \gamma)^{-1} > 1, \quad D \approx C(2\gamma/\pi)^\gamma \quad (3)$$

where the anomalous dimension $\gamma \approx 0.41$ at LEP energies in this approximation and $C \approx 2.5527$.

Analytic results for the realistic case of quark jets with running α_s have been derived for moments of the multiplicity distributions $R_q = \langle n(n-1) \dots (n-q+1) \rangle$

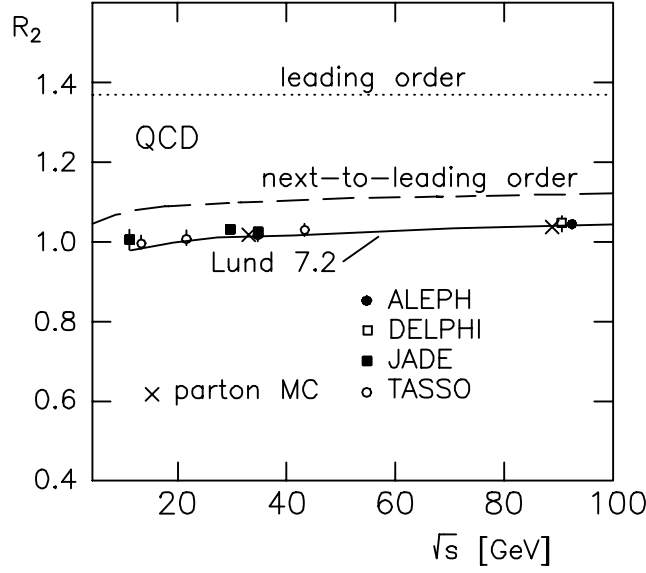


Figure 3: Two particle multiplicity moment $R_2 = \langle n(n-1) \rangle / \langle n \rangle^2$ vs. CM energy. The QCD results in leading order (DLA), NLO²¹ and from parton MC (HERWIG) in comparison with experimental data.¹⁴

$\langle n \rangle^2$. These normalized quantities are again infrared safe. The QCD prediction on R_2 in comparison with experimental data are shown in Fig. 3. The DLA result at infinite energies is $R_2 = \frac{11}{8}$. The next-to-leading order result²¹

$$R_2 = \frac{11}{8}(1 - \chi\sqrt{\alpha_s}) \quad (4)$$

with $\chi = 0.55$ reduces the moment by $\sim 30\%$ but still differs from data by $\sim 10\%$. We have calculated this moment also with the MC method (using the program HERWIG¹⁰ at the parton level[§]) which fully takes into account energy momentum conservation. This result finally matches the data and confirms PHD for an infrared safe quantity.

3. Inclusive One-Particle Distributions and the LPHD Hypothesis

3.1 Momentum Spectra

One defines the logarithmic variable $\xi = \ln(P/k) \equiv \ln(1/x)$ for a particle of momentum k emitted from a primary parton P ; $0 \leq \xi \leq Y$ with $Y = \ln(P\Theta/Q_0)$. The asymptotic DLA results are known for fixed α_s ⁶

$$\frac{dn}{d\xi} \sim \left(\frac{Y-\xi}{\xi}\right)^{1/2} I_1\left(2\gamma_o\sqrt{\xi(Y-\xi)}\right) \quad (5)$$

$$\approx \exp(-2\gamma_o(\xi - \frac{Y}{2})^2/Y) \quad (6)$$

[§]We take the perturbative cascade without $g \rightarrow q\bar{q}$ splitting at the end of the cascade and choose parameters $\Lambda = 0.15$ GeV, $m_q = m_g = 0.32$ GeV.

and for running α_s where one obtains in Gaussian approximation^{22,4}

$$\frac{dn}{d\xi} \sim \frac{\bar{n}}{((Y + \lambda)^{3/2} - \lambda^{3/2})^{\frac{1}{2}}} \exp\left(-\frac{3\beta(\xi - \frac{Y}{2})^2}{(Y + \lambda)^{3/2} - \lambda^{3/2}}\right) \quad (7)$$

with $\lambda = \ln(Q_0/\Lambda)$, β defined above. The constant α_s result (6) can be recovered from this by the formal limit $\beta, \lambda \rightarrow \infty$, $\beta/\sqrt{\lambda} = \gamma_0$ fixed. This Gaussian shape, known as “hump-backed plateau”, is characteristic of the destructive soft gluon interference resulting in the suppression of small momenta. The maximum occurs for $\xi^* = \frac{Y}{2}$. The width behaves like

$$\begin{aligned} \sigma^2 &\sim Y && \text{for } \alpha_s \text{ fixed} \\ \sigma^2 &\sim Y^{\frac{3}{2}} && \text{for } \alpha_s \text{ running} \end{aligned} \quad (8)$$

So the running of α_s influences the shape of the distribution. As Y depends on Q_0 this distribution is not infrared safe. However one can consider a high energy limit using the rescaled variable¹¹

$$\zeta = \frac{\xi}{(Y + \lambda)} \equiv \frac{\ln(P/k)}{\ln(P\Theta/\Lambda)} \quad (10)$$

In great analogy to the case of angular correlations³⁴ to be discussed below we can construct a quantity with a scaling limit and obtain from (7)

$$\frac{\ln dn/d\xi}{\ln \bar{n}} \simeq 1 - \frac{3(\zeta - \zeta_0/2)^2}{2(1 - (1 - \zeta_0)^{\frac{3}{2}})} \rightarrow 1 - \frac{3}{2}(\zeta - \frac{1}{2})^2 \quad (11)$$

where the last limit holds for large Y , $\zeta_0 = Y/(Y + \lambda) \rightarrow 1$. So this quantity becomes infrared safe for high energies.

Results in higher orders have been obtained by the St. Petersburg group¹¹ (for a review of various approximations, see ref. 6). Again the corrections to the DLA are sizable. For example, the position of the maximum ξ^* is shifted away by an amount of $O(\sqrt{\alpha_s})$

$$\xi^* = Y\left(\frac{1}{2} + a\sqrt{\frac{\alpha_s(Y)}{32N_c\pi}} - a^2\frac{\alpha_s(Y)}{32N_c\pi} + \dots\right), \quad a = \frac{11}{3}N_c + \frac{2N_f}{3N_c^2} \quad (12)$$

In the application to experiment these authors proposed the hypothesis of “Local Parton Hadron Duality”¹¹

$$\left.\frac{dn}{d\xi}\right|_{hadron} = const \left.\frac{dn}{d\xi}\right|_{parton, Q_0=m_h} \quad (13)$$

a proportionality of the spectra of hadrons to the one of partons for a cascade evolved down to a hadronic mass, $Q_0 = m_h$, which is taken typically as m_π . Of course, such

Figure 4: Distributions in $\xi = \ln 1/x_p$ of charged hadrons at different energies compared with the analytical MLLA formula and a distorted Gaussian for parton cascade evolved down to a mass of 250 MeV, taken from Ref.²³

a hypothesis cannot be correct for all observables (for example, the mass spectrum of two partons does not show a ρ -meson), but it is interesting to explore its validity for sufficiently inclusive quantities. The relation (13) is tested in Fig. 4, where on the r.h.s. the “limiting spectrum” in MLLA is inserted which is obtained from the general formula by letting $Q_0 = m_h \rightarrow \Lambda$. For charged particle spectra an effective hadron mass of $m_h = 253$ MeV is taken. It is remarkable how well the shape of the distribution and its energy evolution is fitted by the theoretical prediction in terms of 2 parameters (m_h, const) for not too small momenta ($k \gtrsim 400$ MeV). A closer inspection of Fig. 4 also shows that the deviation from the DLA prediction (7) both in the position of the peak ξ^* and in the energy dependence are well supported.⁶

Recently it has been questioned²⁴ as to what extent this result provides evidence for the soft gluon interference of QCD. A model has been considered (JETSET 7.3) with a parton cascade, cut off at $Q_0 \sim 1$ GeV, either including or not including the soft gluon coherence, followed by string hadronization. The parameters of the hadronization model are adjusted in both cases so as to reproduce the main features of the data. In Fig. 5 one can see the ξ -spectra of gluons, from the coherent calculation with Gaussian shape and the non-coherent calculation with a higher particle density towards larger ξ , i.e. smaller momenta. Both models after hadronization yield the same spectra for charged particles which are also in good agreement with data on charged particles of Fig. 4. Therefore within this hadronization model, as stated,²⁴ no evidence can be claimed from the measurements in favor of the soft gluon inter-

Figure 5: Distributions in $\xi = \ln 1/x_p$ from the string model (JETSET 7.3) at the parton level (“Gluons”) with and without the color coherence of the QCD included, and for charged particles (C^\pm) of the final hadronic state (from ref.24).

ference effect. On the other hand, evolving the parton cascade further according to QCD from $Q_0 \sim 1$ GeV to $Q_0 = m_h$, only the gluon distribution for the coherent case would approach the data (as is asserted by Fig. 4). This example nicely demonstrates the predictive power of the LPHD hypothesis and the similarity of parton and hadron spectra at comparable scales. On the other hand hadronization models have considerable flexibility to bring quite different theoretical schemes at the parton level into agreement with the data. In particular, the LPHD relation (13) is a consequence of the string model only for a special set of model parameters.

3.2 Hadron mass effects

In a more speculative application of the LPHD hypothesis the distribution of heavier particles of mass M is given as in Eq. (13) with the cutoff $Q_0 = M > \Lambda$, whereas for pions $Q_0 = m_\pi \approx \Lambda$. In the DLA the peak position $\xi^* = \frac{Y}{2}$, so for a heavier particle the peak is shifted by

$$\Delta\xi = -\frac{1}{2} \ln \frac{M}{m_\pi} \quad (14)$$

with respect to the pion independent of energy. The numerical studies of the MLLA equation²⁵ conform this energy independence and $\Delta\xi = f(M/\Lambda)$. In Fig. 6a one can see that the data for π^0, η are indeed separated by an energy independent amount. The peak position ξ^* at LEP-energies for various hadrons are shown in Fig. 6b together

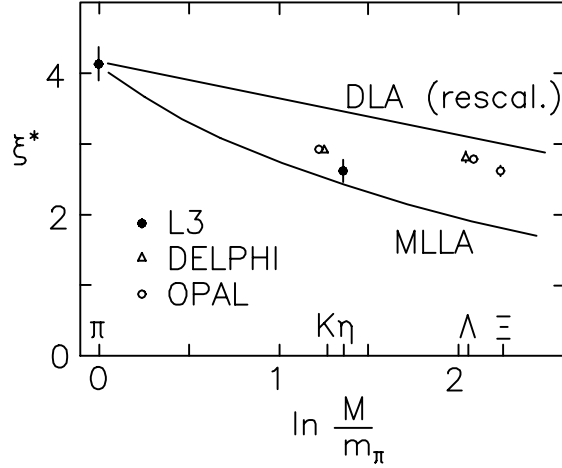


Figure 6: Peak position ξ^* of the distribution in $\xi = \ln(P/k)$ vs. CM energy for π^0 and η^{26} (left side); ξ^* vs. hadron mass M at LEP energies compared with predictions from DLA and MLLA. Data from compilation²⁷ (right side).

with the prediction from DLA, Eq. (14) and MLLA extracted from the published results.²⁵ The ξ^* value drops when going from π to K/η similarly to the MLLA prediction but then saturates: the relation $Q_0 = M$ does not work well for heavier particles.

4. Two Particle Correlations

4.1 Momentum Correlations

The normalized correlation function is defined by

$$R_2(\xi_1, \xi_2) = \rho^{(2)}(\xi_1, \xi_2) / \rho^{(1)}(\xi_1) \rho^{(1)}(\xi_2) \quad (15)$$

in terms of the n -particle density $\rho^{(n)}$. It has been calculated in NLO as an expansion in the arguments up to second order²⁸ and is found to depend only on the rescaled observables $\zeta_i = \xi_i / (Y + \lambda)$ at high energies. Alternatively one could choose the rescaled observable ξ/ξ^* as $\xi^* = Y/2$ in DLA. In Fig. 7 we show $R_2(\xi_1, \xi_2)$ for $\xi_1 = \xi_2$ vs. ξ/ξ^* (where $\xi \equiv \xi_1$) at the parton and hadron level as we obtained from the HERWIG MC at two different primary quark energies.

Contrary to the integrated moment F_2 (see Fig. 3) PHD does not work well for the differential moment but it improves with increasing energy, so one may speak of asymptotic PHD.

4.2 Azimuthal angle correlations

Energy-multiplicity-multiplicity correlations in the azimuthal angle around the jet direction have been calculated in DLA³⁰ and next-to-leading order.³¹ The NLO calculations for large relative angles ($\varphi = \pi$) differ from the MC results at the parton

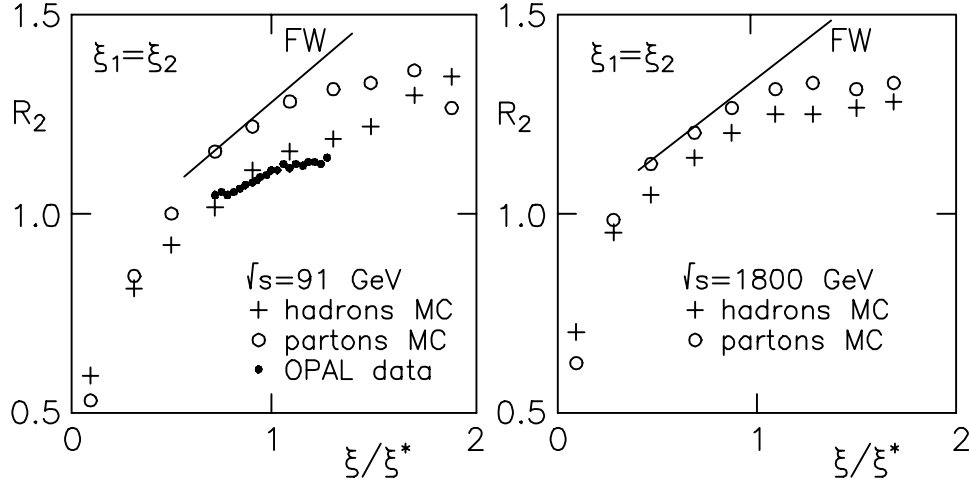


Figure 7: Two-particle momentum correlation function $R_2(\xi_1, \xi_2)$ for $\xi_1 = \xi_2$ vs. ξ/ξ^* , where $\xi \equiv \xi_1$, and ξ^* is the peak position of $\rho^{(1)}$, for hadrons and partons from the HERWIG MC together with the analytical result in linear approximation by Fong and Webber ($\Lambda=255$ MeV). Also shown are the OPAL data.²⁹

level by $\sim 10\%$ but the experimental data follow the MC results closely for not too small relative angles φ ³² in favor of PHD. The difference between coherent and incoherent models is rather small, typically about 5%.

4.3 Polar angle correlations

The correlations in the relative polar angle ϑ_{12} of two partons within the forward cone of half opening angle Θ have been derived in DLA.^{33,34} This is a special case of n -particle angular observables $h^{(n)}(\delta, \vartheta, P)$, like multiplicity moments, to be discussed below. For such quantities the leading asymptotic behavior is given by

$$h^{(n)}(\delta, \vartheta, P) \sim \exp(2\beta\sqrt{\ln(P\vartheta/\Lambda)}\omega(\varepsilon, n)) \quad (16)$$

$$\varepsilon = \frac{\ln(\vartheta/\delta)}{\ln(P\vartheta/\Lambda)} \quad (17)$$

Because of $\delta \gtrsim Q_0/P \gtrsim \Lambda/P$ the rescaled angular variable fulfils $0 \leq \varepsilon \leq 1$. The scaling function $\omega(\varepsilon, n)$ is known³³ and can be expanded for small ε like

$$\omega(\varepsilon, n) = n - \frac{1}{2} \frac{n^2 - 1}{n} \varepsilon + \dots \quad (18)$$

and for large n like

$$\omega(\varepsilon, n) = n\sqrt{1 - \varepsilon} + O\left(\frac{1}{n}\right) \quad (19)$$

For the 2-particle correlation within the cone of half opening Θ the quantity

$$\hat{r}(\vartheta_{12}, \Theta, P) = \rho^{(2)}(\vartheta_{12}, \Theta, P) / \bar{n}^2(\Theta, P) \quad (20)$$

is considered where \bar{n} is the multiplicity in the forward cone. In DLA one obtains the asymptotic prediction

$$\hat{r}(\vartheta_{12}, \Theta, P) \sim \exp \left(2\beta \sqrt{\ln(P\Theta/\Lambda)} (\omega(\varepsilon, 2) - 2) \right) \quad (21)$$

An interesting property of this result is the “ ε -scaling”. Up to a known prefactor in the exponent the correlation function depends on the three variables $\vartheta_{12}, \Theta, P$ only through the single rescaled angular variable ε . This scaling property is checked by the MC calculation at the parton level in Fig. 8 which shows the ε -dependent part of the exponent in (21) vs. ε . For sufficiently small $\varepsilon \lesssim 0.5$ this scaling property is indeed well satisfied for $P \gtrsim 20$ GeV. Eq. (21) can also be seen to reproduce the trend of the MC data. Some nonasymptotic corrections within DLA different for quark and gluon jets, are also known.³⁴ In Fig. 8 we have adjusted the overall normalization because this is a nonleading effect.

For small ε with (18) the correlations become asymptotically power behaved

$$\hat{r}(\vartheta_{12}) = (\Theta/\vartheta_{12})^{-\frac{3}{2}\gamma_o(P\Theta)} \quad (22)$$

and this can be related to the selfsimilarity of the jet cascade. This power law holds asymptotically in the full angular region for fixed α_s , so the curvature in Fig. 8 in the asymptotic curve reflects the running of α_s .

A comparison of the parton and hadron MC reveals that in the region with scaling $\varepsilon \lesssim 0.5$ there is also PHD (in the MC). This region is again characterised by its independence of Q_0 in confirmation of the general rule. A preliminary result from the DELPHI collaboration,³⁵ also presented at this conference, supports indeed PHD for this observable, i.e. the close similarity of the experimental and parton MC data (as $Q_0 > m_h$ in the MC we talk here about PHD and not LPHD). Furthermore the first evidence for ε -scaling in the opening angle Θ (for $30^\circ \leq \Theta \leq 60^\circ$) has been presented.

Another interesting aspect is the sensitivity to the soft gluon interference which is most naturally observed in the polar angle correlations. This is demonstrated by an analysis with L3 data³⁶ considering the Particle-Particle-Correlations (PPC). They are defined like the well-known energy-energy correlations³⁷ but without the energy weights in the double sum over particle pairs. Likewise defined is the asymmetry PPCA (ϑ_{12}) = PPC ($180^\circ - \vartheta_{12}$) - PPC(ϑ_{12}). Disregarding the fluctuations of multiplicity N_{ch} this quantity is related to our correlation function like $\text{PPCA}(\vartheta_{12}) \approx -(\rho^{(2)}(\vartheta_{12}) - \rho_{\text{uncorr.}}^{(2)}(\vartheta_{12}))/\bar{n}^2$.

In Fig. 9 results are shown from the JETSET MC for the angular asymmetry PPCA which varies strongly for small ϑ_{12} if angular ordering (AO) is properly included as required by QCD. The data follow closely the AO-case. The sharp dip at small ϑ_{12} is related to the peak in $\rho^{(2)}(\vartheta_{12}) \sim 1/\vartheta_{12}$ in DLA,³³ but also Bose-Einstein correlations could be important in this region.

The angular ordering condition implies that a soft gluon is emitted from a parton 1 only within an angular cone limited by the next color connected parton

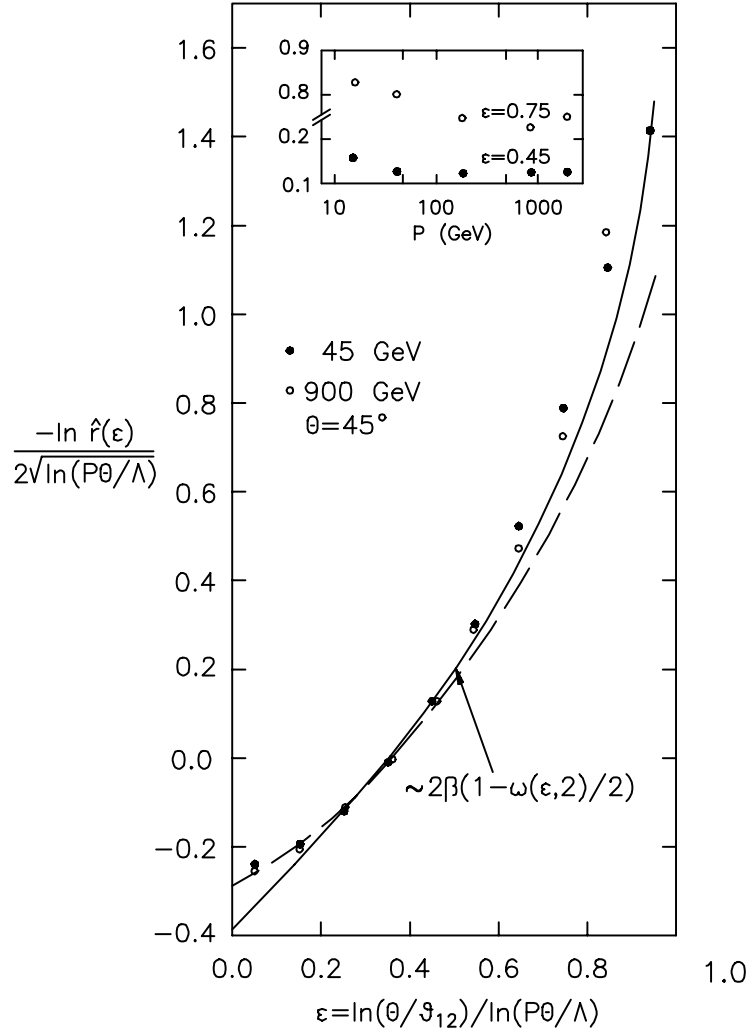


Figure 8: Rescaled 2-particle polar angle correlation vs. scaling variable ε for different primary energies P and for fixed cone opening Θ (with respect to the sphericity axis) from the parton MC (HERWIG). The full curve represents the high energy limit of the DLA; the dashed curve the prediction for quark jets at 45 GeV; the normalization of the curves is adjusted. The insert shows the energy dependence of the same quantity for fixed ε ; from Ref.³⁴

($\vartheta_{12} \leq \vartheta_{1 \text{ next}}$). We may estimate roughly $\vartheta_{1 \text{ next}} \sim \bar{\vartheta}_{12} \sim \Theta/\sqrt{n}$ which corresponds to about $1/\sqrt{15}$ rad $\sim 15^\circ$. One expects the emission within this angular region to be enhanced, outside to be suppressed in comparison to the not ordered case. Interestingly, such an effect is indeed seen in Fig. 9 (note that $\text{PPCA} \sim -\rho^{(2)}$), so this interference effect between gluons is actually visible between hadrons in the region $15\text{-}50^\circ$. This consideration also makes clear that the effect of angular ordering is most clearly seen in the polar angle (and not in the azimuthal angle or between momenta).

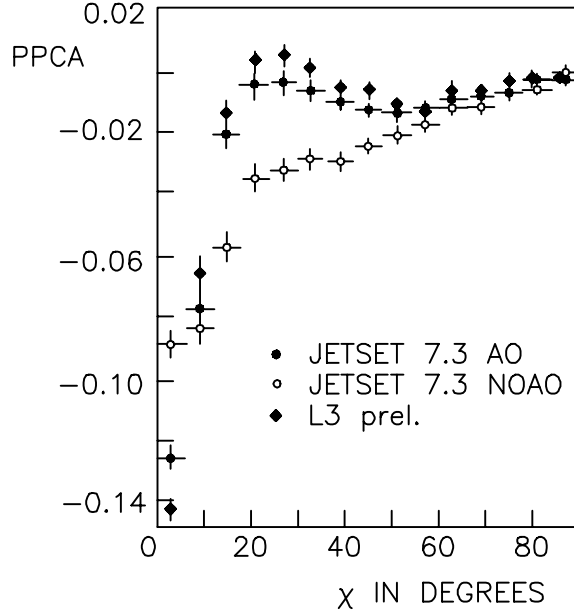


Figure 9: Particle Particle Correlation Asymmetry vs. relative polar angle $\chi \equiv \vartheta_{12}$ from L3 experiment³⁶ in comparison with the string MC with angular ordering (AO) and without (NOAO).

5. Angular Correlations of General Order n

The general n -particle cumulant correlation function has also been studied in DLA.³⁴ Here we discuss only as application the integral over the correlation function in certain angular regions. First we discuss the sidewise ring where the polar angles ϑ_i with respect to the initial parton are within the range $\vartheta - \delta \leq \vartheta_i \leq \vartheta + \delta$, second the sidewise cone centered at a polar angle ϑ and half opening δ . We refer to these configurations as dimension $D = 1$ and $D = 2$ cases according to the phase space volume δ^D . The factorial multiplicity moments are obtained from

$$f^{(n)}(\vartheta, \delta) = \int \rho^{(n)}(\Omega_1, \dots, \Omega_n) d\Omega_1 \dots d\Omega_n \quad (23)$$

or normalized $F^{(n)} = f^{(n)}/\bar{n}^n$. In analogy the cumulant moments are constructed from the cumulant (connected) correlation functions and are related to the factorial moments³⁸ (i.e. $C_2 = F_2 - 1$, etc.).

At high energies one obtains in DLA^{33,39,40}

$$C^{(n)}(\vartheta, \delta) = (\vartheta/\delta)^{\varphi_n}, \varphi_n = D(n-1) - 2\gamma_0(P\vartheta)(n - \omega(\varepsilon, n))/\varepsilon \quad (24)$$

In leading approximation the difference between factorial and cumulant moments vanish.[¶] Corrections in the MLLA are also given³⁹ and amount to typically 10%.

[¶]The formula (24) is given for the cumulant moments in ref.³³ and for the factorial moments in refs.^{39,40}

In the limit of small ε (sufficiently large opening angles δ) one can use the linear approximation for $\omega(\varepsilon, n)$ (18) and (24) becomes a power law with

$$\varphi_n = D(n-1) - (n - \frac{1}{n})\gamma_0(P\vartheta) \quad (25)$$

This power behaviour reflects the fractal structure of the selfsimilar cascade. In this limit, the behavior of moments is also independent of Q_0 , i.e. infrared safe. For small angles $\delta \sim Q_0/P$ the above asymptotic formula is inappropriate and strong sensitivity to Q_0 appears.

This type of power behavior was studied intensively in the last years in the context of “intermittency”.⁴¹ Whereas these phenomenological studies concentrate mainly on the small angle region the power behavior in QCD occurs only for the fully developed cascade at sufficiently large angles (small ε).

As in the case of two particle correlations we can exhibit the ε -scaling by considering the quantity

$$-\hat{C}^{(n)} = -\frac{\ln[(\delta/\vartheta)^{D(n-1)}C^{(n)}]}{n\sqrt{\ln(P\vartheta/\Lambda)}} \quad (26)$$

in the high energy limit. One obtains

$$-\hat{C}^{(n)} \sim 2\beta(1 - \omega(\varepsilon, n)/n) \quad (27)$$

$$\approx 2\beta(1 - \sqrt{1 - \varepsilon}) \quad (28)$$

where the last approximation follows for the large n limit (19) and is independent of n .

In Fig. 10 we show the quantity $-\hat{C}^{(2)}$ for the ring ($D = 1$) from (26) for different energies from the parton MC. There is still considerable scale breaking at small ε but the data points approach at high energies the DLA result (27). We also show in Fig. 10 the analogous results for factorial moments (definition as in (26)). In this case the ε -scaling sets is already at low energies with an ε -dependence as in (27). Note that the absolute scale as well as the difference between factorial and cumulant moments is of nonleading order in DLA.

An interesting aspect of these results is the universal behavior of the observables $\hat{C}^{(n)}$ for different n, D and also of the quite different observable $\hat{r}(\varepsilon)$. The observables $\hat{r}(\varepsilon)$ and $\hat{C}^{(2)}$ in Figs. 8 and 10 are determined from different parts of phase space but nevertheless approach the same asymptotic limit. Such a similarity is a characteristic property of the QCD cascade. The comparison of parton and hadron MC shows again that PHD works well in the model for not too large ε near 1.³⁴

6. Clans

Clans are defined⁴² as group of particles of common ancestor. The clans are independently produced and therefore the number of clans in an event follow a Poisson

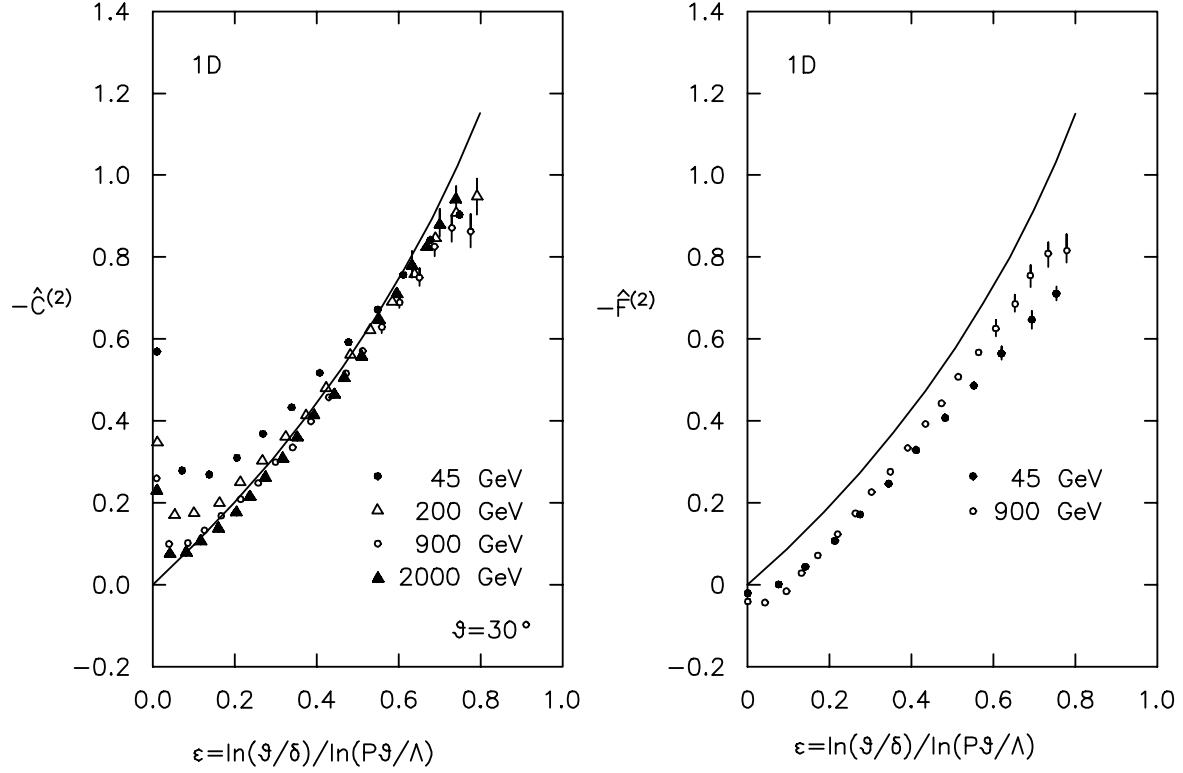


Figure 10: (a) Rescaled cumulant moments for the ring ($D=1$) as defined in Eq.(26) from the parton MC for different jet momenta P in comparison with the asymptotic prediction Eq.(27), (b) same as (a) but for factorial moments.

distribution. With the assumption of a logarithmic distribution of particles in a clan one obtains a negative binomial distribution of particles, which describes the data in a good approximation.

The analysis of multiplicity distributions in symmetric rapidity windows $|y| < y_c$ has revealed the interesting result that the average number of clans $\bar{N}(y_c, \sqrt{s})$ at fixed CM energy \sqrt{s} grows linearly with y_c for a large range of y_c before it bends if y_c approaches the full phase space y_{fps} . There is only a weak energy dependence of this phenomenon.

One may think of the clans as the jets which evolve from the gluons radiated off the primary partons in the collision in a Bremsstrahlung fashion with a Poisson distribution. This connection between parton and hadron level has been studied in hadronization models. In particular, the $1/k$ parameter of the negative binomial distribution was found about equal at parton and hadron level for $\sqrt{s} \geq 200$ GeV whereas the multiplicity \bar{n} was larger for hadrons than for partons. It is interesting to note that $1/k$ parameter determines fully the normalized factorial moments. They are expected to be infrared safe as it is known for the full interval (see 2.2 and Fig.

3). On the other hand \bar{n} is clearly Q_0 dependent and therefore different at parton and hadron level. In a generalization of these findings it has been suggested that the differential rapidity distributions $\rho^{(n)}(y_1 \dots y_n)$ at the parton and hadron level are proportional (“Generalized Local Parton Hadron Duality”⁴³). This relation certainly works best if the cutoff Q_0 is close to the hadron mass. Otherwise there will be different kinematic limits. In that case there may be a better duality for the rescaled rapidities y/y_{max} .

An interesting scaling property in terms of a rescaled rapidity has recently been found⁴⁴ for the clan multiplicity. The multiplicity ratio $\pi^* = \bar{N}(y_c, \sqrt{s})/\bar{N}(y_{fps}, \sqrt{s})$ is calculated analytically in a simplified version of the QCD parton shower. This quantity scales well in the rescaled rapidity $y_c^* = y_c/y_{fps}$

$$\pi^*(y_c^*, \sqrt{s}) \approx \pi^*(y_c^*) \quad (29)$$

in the studied range $50 < \sqrt{s} < 500$ GeV and approaches in the very high energy limit

$$\pi^*(y_c^*, \sqrt{s}) \simeq y_c^* + O\left(\frac{1}{\ln \ln \sqrt{s}}\right) \quad (30)$$

where the approach to this limit is very slow.

7. Limitations of Parton Hadron Duality

For the inclusive observables discussed so far the PHD concept seems to work rather well as seen from experimental data or suggested by MC calculations. We have, finally, to discuss where we expect or observe the limitations.

We clearly expect deviations in the short range correlations due to resonance effects which occur at the hadron but not at the parton level, i.e. for masses $M_{ij} \lesssim 1 - 1.5$ GeV. This causes a violation of PHD, for example, in the correlation function $r(\varepsilon)$ for $\varepsilon \rightarrow 1$ or $\vartheta_{12} \rightarrow Q_0/P$. A recent example of this type has been presented by the OPAL collaboration.⁴⁵ The measured ratio of sub-jet multiplicities in two- and three-jet events deviates from the QCD prediction⁴⁶ at the parton level below a resolution scale of ~ 2 GeV. As this scale is a bit large it would be desirable to understand better the reasons for the sudden change in slope at the hadron level (charm production?). In any case the discrepancy between data and theory is only of the order of 10%.^{||}

Another interesting limit where PHD may fail and is expected to fail in standard hadronization models is the quasielastic limit in e^+e^- annihilation with a large rapidity gap. Such events at the parton level correspond essentially to $e^+e^- \rightarrow q\bar{q} + (\text{few soft gluons})$. The probability for this state is given by the Sudakov form factor for no radiation into this angular interval. With PHD the parton final state would transform into a similar final state with large rapidity gap (see Fig. 11).

In the standard hadronization models there is a color field between the separated partons which would decay into many hadrons of small p_T . Assuming an

^{||}I would like to thank T. Sjöstrand for bringing this result to my attention and for correspondence.

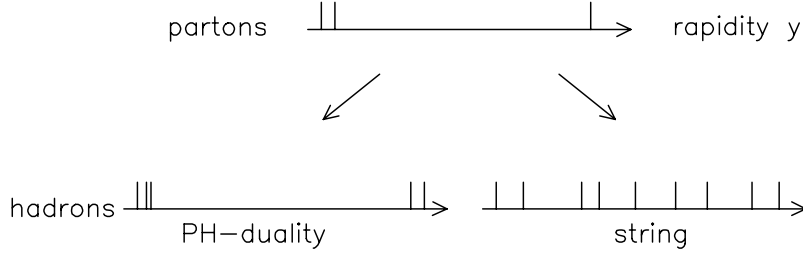


Figure 11: Hadronization of a quasi-exclusive partonic state yields a different hadronic final state according to Parton Hadron Duality and the string model.

independent emission of particles or clusters with rapidity density c the probability for a gap of length Δy is⁴⁷ $P = \exp(-c\Delta y)$, so there is this additional suppression to obtain events with a large rapidity gap. Then there is no PHD in the standard hadronization models in this limit. If an effect of this type was observed it would imply color bleaching earlier in the cascade than usually thought, some kind of exclusive PHD.⁴⁸

An effect of this type has actually been seen in the MC simulation of the 2-jet rate for small resolution scales y_{cut} at parton and hadron level.⁴⁹ For $y_{\text{cut}} \sim 10^{-4}$ (K_T scale ~ 1 GeV) the rate for the hadronic 2-jet events is found about hundred times larger than for the partonic ones.

8. Conclusions

It is quite remarkable that the QCD calculations on the parton cascade match the experimental data and this suggests indeed a rather soft hadronization mechanism. The scheme of PHD is well-defined and economic with the only parameter Λ for infrared safe quantities, and the additional quantity Q_0 otherwise. We have considered here mainly inclusive infrared sensitive quantities.

1. *PHD and LPHD.* As a general rule, if the DLA result is independent of Q_0 (after appropriate normalization) then the hadronization corrections are small (multiplicity moments, angular observables for small ε). There are cases where the Q_0 dependence disappears only asymptotically, then also PHD does the same (momentum correlations). In some cases the nonasymptotic corrections are large (cumulant angular correlations $\hat{C}(\varepsilon)$). The LPHD hypothesis with $Q_0 = m_h$ is successful for momentum spectra of the light hadrons (not well for heavier hadrons), but no other application has been provided so far.

2. *Rescaled variables* appear naturally in the description of the QCD cascade: $n/\bar{n}, \zeta, \varepsilon, y_c^*$. Especially the recently introduced angular variable $\varepsilon(\delta, \vartheta, P)$ provides a new type of scaling predictions for the QCD cascade with two redundant variables ϑ, P .^{33,34} First results presented at this meeting look promising for the ϑ -independence.³⁵

3. *Soft gluon interference* is taken into account by the angular ordering prescription. There is evidence from the shape of the hump backed plateau (see Figs. 4,5) and the multiplicity rise, but most sensitive are correlations in the relative polar angle ϑ_{12} which are enhanced and suppressed at small and large relative angles.

4. *Running α_s* . The distributions in various observables are markedly different for a fixed or running α_s calculation, as in case of momentum spectra and in particular angular observables which are power behaved for fixed α_s .

In this review we have considered results from e^+e^- annihilations but interesting results on color coherence phenomena are coming now also from the hadron collider at Fermilab⁵⁰ and at this conference from HERA.⁵¹

Analytical QCD calculations on multiparticle final states can reveal interesting scaling and universality patterns which provide new insights into the intrinsic structures of jets. With sufficient care in the selection of infrared safe quantities there is a promising path in the calculation of multiparticle phenomena from basic principles of QCD. Also the extension towards small scales $Q_0 \sim m_h$ is worth pursuing. A satisfactory understanding though of why PHD or LPHD works so well is not really known.

9. References

- [1] V.N. Gribov, L.N. Lipatov, *Sov. J. Nucl. Phys.* **15** (1972) 438, 675.
- [2] G. Altarelli, G. Parisi, *Nucl. Phys.* **B126** (1977) 298.
- [3] K. Konishi, A. Ukawa, G. Veneziano, *Nucl. Phys.* **B157** (1979) 45.
- [4] A. Bassetto, M. Ciafaloni, G. Marchesini, *Phys. Rep.* **100** (1983) 202.
- [5] Yu.L. Dokshitzer, V.A. Khoze, A.H. Mueller, S.I. Troyan, *Rev. Mod. Phys.* **60** (1988) 373.
- [6] Yu.L. Dokshitzer, V.A. Khoze, A.H. Mueller, S.I. Troyan, *Rev. Mod. Phys.* **60** (1988) 373, *Basics of Perturbative QCD*, Editions Frontières, Gif-sur-Yvette CEDEX-France (1991).
- [7] D. Amati, G. Veneziano, *Phys. Lett.* **83** (1979) 87.
- [8] Z. Kunszt, P. Nason, G. Marchesini, B.R. Webber, "Z Physics at LEP1", Ed. G. Altarelli et al., Vol. 1, p. 373 (1989), CERN 89-08.
- [9] B. Andersson, G. Gustafson, G. Ingelman, T. Sjöstrand, *Phys. Rep.* **97** (1983) 33; T. Sjöstrand, M. Bengtsson, *Comp. Phys. Comm.* **43** (1987) 367.
- [10] G. Marchesini, B.R. Webber, *Nucl. Phys.* **B238** (1984) 1; **B310** (1988) 461; G. Marchesini, B.R. Webber, G. Abbiendi, I.G. Knowles, M.H. Seymour, L. Stanco, *Comp. Phys. Comm.* **67** (1992) 465.
- [11] Ya. I. Azimov, Yu. L. Dokshitzer, V.A. Khoze, S.I. Troyan, *Z. Phys.* **C27** (1985) 65; **C31** (1986) 21.
- [12] A. Bassetto, M. Ciafaloni, G. Marchesini, A.H. Mueller, *Nucl. Phys.* **B207** (1982) 189.

- [13] A.H. Mueller, *Nucl. Phys.* **B213** (1983) 85.
- [14] D. Decamp et al., (ALEPH coll.), *Phys. Lett.* **B273** (1991) 181.
- [15] A. Bassetto, M. Ciafaloni, G. Marchesini, *Nucl. Phys.* **B163** (1980) 477
- [16] Z. Koba, H.B. Nielsen, P. Olesen, *Nucl. Phys.* **B40** (1972) 317.
- [17] A.M. Polyakov, *Sov. Phys. JETP* **32**, 296 (1971); **33** (1971) 850.
- [18] F. Cuyper, K. Tesima, *Z. Phys.* **C54** (1992) 87.
- [19] Yu. L. Dokshitzer, *Phys. Lett.* **B305** (1993) 295.
- [20] P. Duclos, J.L. Meunier, Institut Non Linéaire de Nice, preprint INLN 94/20 (1994).
- [21] E.D. Malaza, B.R. Webber, *Phys. Lett.* **B149** 501.
- [22] A.H. Mueller, 10th SLAC Summer Institute on Particle Physics, August 1982.
- [23] M.Z. Akrawy et al. (OPAL coll.) *Phys. Lett.* **247** (1990) 617.
- [24] E.R. Boudinov, P.V. Chliapnikov, V.A. Uvarov *Phys. Lett.* **B309** (1993) 210.
- [25] Yu.L. Dokshitzer, V.A. Khoze, S.I. Troyan, Perturbative QCD workshop, Lund, May 1991, preprint LU-TP-91-12.
- [26] O. Adriani (L3 coll.), *Phys. Lett.* **B286** (1992) 403.
- [27] M.N. Kienzle Focacci, Proc. XXVI Int. Conf. High Energy Physics, August 1992, Dallas, Texas, Ed. J. R. Sanford, American Institute of Physics (1993).
- [28] C.P. Fong, B.R. Webber, *Nucl. Phys.* **B355** (1991) 54.
- [29] P.D. Acton et al. (OPAL coll.), *Phys. Lett.* **B287** (1992) 401.
- [30] Yu. L. Dokshitzer, V.A. Khoze, G. Marchesini, B.R. Webber, *Phys. Lett.* **B245** (1990) 243.
- [31] Yu. L. Dokshitzer, G. Marchesini, G. Oriani, *Nucl. Phys.* **B387** (1992) 675.
- [32] P.D. Acton et al. (OPAL coll.), *Z. Phys.* **C58** (1993) 207.
- [33] W. Ochs, J. Wosiek, *Phys. Lett.* **B289** (1992) 159; *Phys. Lett.* **B304** (1993) 144.
- [34] W. Ochs, J. Wosiek, “*Angular structure of QCD jets*”, MPI-preprint in preparation; W. Ochs, to be publ. in Proc. Workshop “*Hot Hadronic Matter: Theory and Experiment*”, June 1994, Divonne-les-Bains, France, Plenum, N.Y., preprint MPI-Ph/94-68; W. Ochs, Proc. Cracow Workshop on Multiparticle Production, “*Soft Physics and Fluctuations*”, Cracow, Poland, May 1993, Eds. A. Bialas et al., World Scientific, Singapore (1994), p.150; J. Wosiek, *Act. Phys. Pol.* **24** (1993) 1027.
- [35] F. Mandl, B. Buschbeck (DELPHI coll.), to be published in Proc. of QCD conference, Montpellier, July 1994, Vienna preprint; see also these proceedings.
- [36] A.A. Syed, thesis Katholieke Universiteit Nijmegen, “*Particle Correlations in Hadronic Decays of the Z-Boson*”, L3-Experiment, 1994; See also W. Kittel in these proceedings.

- [37] C.L. Basham, L.S. Brown, S.D. Ellis, S.T. Love, *Phys. Rev.* **D17** (1977) 2298.
- [38] E.A. De Wolf, I.M. Dremin, W.K. Kittel, *Usp. Fiz. Nauk* **163** (1993) 3; “*Scaling Laws for Density Correlations and Fluctuations in Multiparticle Dynamics*”, Nijmegen preprint HEN-362 (1993) and Brussels preprint IIHE-ULB-VUB-93-01.
- [39] Yu. L. Dokshitzer, I. Dremin, *Nucl. Phys.* **B402** (1993) 139.
- [40] Ph. Brax, J.L. Meunier, R. Peschanski, *Z. Phys.* **C62** (1994) 649.
- [41] A. Bialas, R. Peschanski, *Nucl. Phys.* **B273** (1986) 703; **B306** (1988) 857.
- [42] A. Giovannini, L. van Hove, *Z. Phys.* **C30** (1986) 391.
- [43] L. van Hove, A. Giovannini, *Acta Phys. Pol.* **B19** (1988) 917.
- [44] R. Ugoccioni, A. Giovannini, S. Lupia, preprint DFTT 7/94, University of Torino.
- [45] R. Akers et al. (OPAL coll.), *Z. Phys.* **C63** (1994) 363.
- [46] S. Catani, Yu. L. Dokshitzer, F. Fiorani, B.R. Webber, *Nucl. Phys.* **B383** (1992) 419.
- [47] L. Stodolsky, *Phys. Rev. Lett.* **28** (1972) 60.
- [48] G. Cohen-Tannoudij, W. Ochs, *Z. Phys.* **C39** (1988) 513.
- [49] B.R. Webber, Proc. “*QCD, 20 years later*”, Aachen, June 1992, eds. P.M. Zerwas, H.A. Kastrup, World Scientific, Singapore (1993).
- [50] F. Abe et al. (CDF coll.), “*Evidence for Color Coherence in $p\bar{p}$ Collisions at $\sqrt{s} = 1.8 \text{ TeV}$* ”, FERMILAB Pub-94/072-E.
- [51] M. Derrick, these Proceedings.

This figure "fig1-1.png" is available in "png" format from:

<http://arxiv.org/ps/hep-ph/9501310v1>

This figure "fig1-2.png" is available in "png" format from:

<http://arxiv.org/ps/hep-ph/9501310v1>